Eur Radiol (2017) 27:518–525
DOI 10.1007/s00330-016-4423-2

HEPATOBILIARY-PANCREAS

Outcome of hypovascular hepatic nodules with positive uptake of gadoxetic acid in patients with cirrhosis

Katsuhiro Sano[1,2] · Tomoaki Ichikawa[1,2] · Utaroh Motosugi[1] · Shintaro Ichikawa[1] · Hiroyuki Morisaka[1,2] · Nobuyuki Enomoto[3] · Masanori Matsuda[4] · Hideki Fujii[4]

Received: 5 October 2015 / Revised: 8 May 2016 / Accepted: 19 May 2016 / Published online: 2 June 2016

Abstract

Objectives To evaluate the longitudinal risk to patients with cirrhosis of hypervascular hepatocellular carcinoma (HCC) developing from hypovascular hepatic nodules that show positive uptake of gadoxetic acid (hyperintensity) on hepatocyte phase images.

Methods In 69 patients, we evaluated findings from serial follow-up examinations of 633 hepatic nodules that appeared hypovascular and hyperintense on initial gadoxetic acid-enhanced magnetic resonance imaging (EOB-MRI) until the nodules demonstrated hypervascularity and were diagnosed as hypervascular HCC. Cox analyses were performed to identify risk factors for the development of hypervascular HCCs from the nodules.

Results The median follow-up was 663 days (range, 110 to 1215 days). Hypervascular HCCs developed in six of the 633 nodules (0.9 %) in five of the 69 patients. The only independent risk factor, the nodule's initial maximum diameter of 10 mm or larger, demonstrated a hazard ratio of 1.25. The one-year risk of hypervascular HCC developing from a nodule was 0.44 %. The risk was significantly higher for nodules of larger diameter (1.31 %) than those smaller than 10 mm (0.10 %, $p < 0.01$).

Conclusions Hypervascular HCC rarely develops from hypovascular, hyperintense hepatic nodules. We observed low risk even for nodules of 10 mm and larger diameter at initial examination.

Key Points

- *Hypervascularization was rare on follow-up examination of hypovascular, hyperintense nodules*
- *The risk of hypervascularization in a nodule increased with large size*
- *Hypovascular, hyperintense nodules require neither treatment nor more intense follow-up*

Keywords Gadoxetic acid-enhanced magnetic resonance imaging · Hepatocellular carcinoma · Hyperintensity · Hypervascularization · Hypovascular hepatic nodules

Abbreviations

AASLD	American Association for the Study of Liver Diseases
AFP	Alpha-fetoprotein
CE-CT	Contrast-enhanced computed tomography
CT	Computed tomography
CTAP	Computed tomography during arterial portography
CTHA	Computed tomography during hepatic arteriography
DN	Dysplastic nodule
HCC	Hepatocellular carcinoma
HP	Hepatocyte phase
MRI	Magnetic resonance imaging
OATP	Organic anion transporter

✉ Katsuhiro Sano
sanokt@saitama-med.ac.jp

[1] Department of Radiology, University of Yamanashi, 1110 Shimokato, Chuo-City, Yamanashi 409-3898, Japan

[2] Department of Diagnostic Radiology, Saitama Medical University International Medical Center, 1397-1 Yamane, Hidaka-City, Saitama 350-1298, Japan

[3] First Department of Internal Medicine, University of Yamanashi, Yamanashi, Japan

[4] First Department of Surgery, University of Yamanashi, Yamanashi, Japan

PIVKA-II	Protein induced by vitamin K absence or antagonist II
T_1WI	T_1-weighted imaging
T_2WI	T_2-weighted imaging

Introduction

Hepatocellular carcinoma (HCC) is a leading cause of cancer-related death worldwide, and early detection decreases the risk of mortality. Typically, early HCCs are small hypovascular nodules, and advanced HCCs are hypervascular [1]. However, the shared features of hypovascularity during the arterial phase of benign dysplastic nodules (DN) and malignant early HCC make their differentiation challenging on conventional dynamic imaging [2, 3].

Gadoxetic acid has been recently launched as a liver-specific contrast agent for magnetic resonance (MR) imaging [4]. Its utility in the diagnosis of HCC is well studied [5–7], especially in the diagnosis of hypovascular HCC [8–12]. Because HCCs typically do not take up gadoxetic acid, it is used as a contrast agent to enhance hepatocyte phase (HP) imaging to differentiate early HCCs from benign nodules even when features of hypervascularity are not apparent [13]. Thus, the evaluation of its uptake on HP images may improve the detection and characterization of hepatic nodules, particularly borderline early-stage nodules, including DN and early HCC. A recent longitudinal observational study demonstrated that hypovascular hepatic nodules that show hypointensity on gadoxetic acid-enhanced HP images are likely to become hypervascular HCCs within a few years [14–19].

Often detected in clinical practice, hypovascular nodules that show hyperintensity on gadoxetic acid-enhanced HP images have been considered benign and have been shown little attention, and little is known about their outcome. However, a recent report suggested that hypovascular HCCs that show iso- or hyperintensity on HP images [20] may require more intense clinical management than the current practice, including treatment or close follow-up. We therefore undertook the evaluation of the longitudinal risk to patients with cirrhosis of developing HCC from hypovascular hepatic nodules that show positive uptake of gadoxetic acid (hyperintensity) on HP imaging.

Materials and methods

Patients

The ethics committee of our institute approved this retrospective cohort study and waived the need for written informed consent.

We selected subjects from 371 consecutive patients with chronic liver disease who underwent gadoxetic acid-enhanced MR imaging (EOB-MRI) at our institution between 1 January and 31 December 2008. Patients were included for study who demonstrated target nodules in the liver on EOB-MRI (detailed later) and had undergone multiphasic contrast-enhanced computed tomography (CE-CT) and blood testing within one month of the initial MR examination and at least one follow-up EOB-MRI before August 2011 (Fig. 1).

We identified 633 hypovascular nodules that showed hyperintensity on HP images in 69 patients (38 men, mean age, 67.1 ± 10.1 years; 31 women, mean age, 69.2 ± 9.4 years) with chronic liver disease from hepatitis C virus infection (46 patients), hepatitis B virus infection (ten patients), both hepatitis B and C infection (one patient), and other causes (12 patients). Maximum nodule diameters measured 5 to 30 mm (mean ± SD, 8.3 ± 3.6 mm).

Clinical data

We recorded the results of blood tests for serum albumin, total bilirubin, alpha-fetoprotein (AFP), and protein induced by vitamin K absence or antagonist II (PIVKA-II), prothrombin ratio, and platelet counts as well as any history of conventional HCC.

MR imaging parameters

EOB-MRI was performed using a 1.5-tesla superconducting system (Signa™ Excite HD, GE Healthcare, Waukesha, WI, USA) and an eight-channel phased array coil. Sequences obtained for all patients (Table 1) included fast spin-echo T_2-weighted imaging (T_2WI), dual echo gradient-echo T_1-weighted imaging (T_1WI), and dynamic gadoxetic acid-enhanced dynamic MR imaging, including hepatic arterial phase and HP images.

Computed tomography parameters

Contrast-enhanced CT was performed using a 16-detector row unit (Aquilion™ 16, Toshiba Medical Systems, Tochigi, Japan) with tube voltage of 120 kVp and tube current of 280 to 400 mA automatically adjusted to the patient's body type. All CE-CT studies utilized nonionic iodine contrast agents (Omnipaque 300, Daiichi-Sankyo, Tokyo, Japan; Iomeron 350, Eisai Global, Tokyo, Japan; andIopamiron 370, Bayer Healthcare Japan, Osaka, Japan) that were rapidly administered intravenously during 30 seconds using a power injector (Auto Enhance A-50; Nemoto Kyorindo, Tokyo, Japan). After initiation of the injection of the contrast agent, images were obtained at 40 seconds during the hepatic arterial phase, 70 seconds at the portal-venous phase, and 180 seconds at the delayed phase.

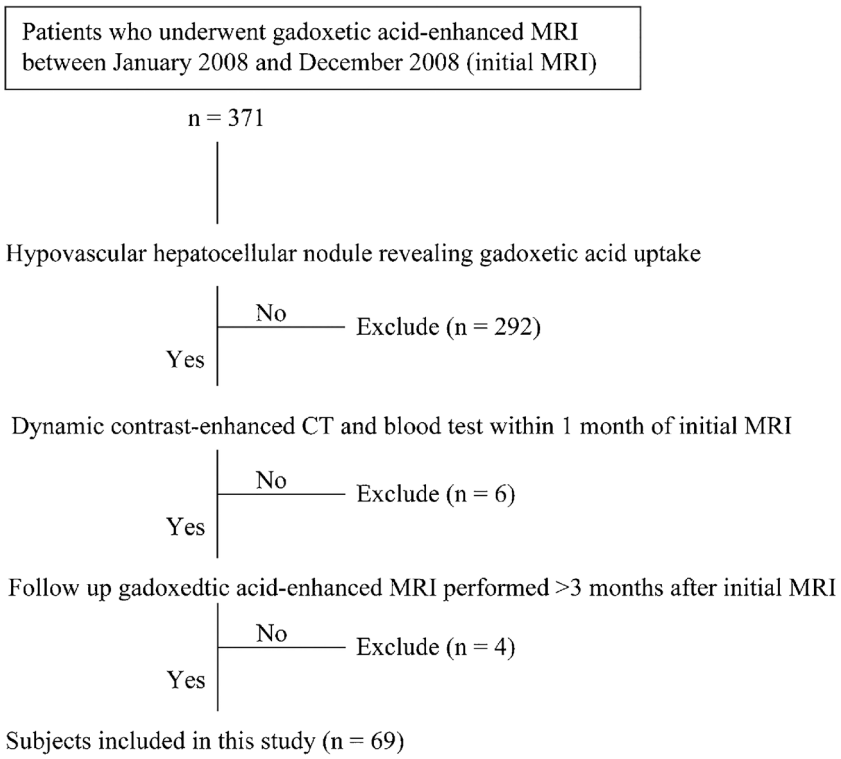

Fig. 1 Flow chart of patient inclusion

Computed tomography during hepatic arteriography (CTHA) and during arterial portography (CTAP) were performed using the same scanner. Images with an effective section thickness of 5 mm were reconstructed every 5 mm to provide contiguous sections. Nonionic contrast agent (Omnipaque 300, Daiichi-Sankyo, Tokyo, Japan; Iomeron 350, Eisai Global, Tokyo, Japan; or Iopamiron 370, Bayer Healthcare Japan, Osaka, Japan) was diluted with saline (20 mL of contrast agent diluted with saline to 60 mL for CTHA and 30 mL of contrast agent diluted with saline to 90 mL for CTAP) and injected into the common hepatic artery (CTHA) or superior mesenteric artery (CTAP). Images were obtained 10 and 35 seconds after initiation of the injection of contrast agent for CTHA and 30 to 35 seconds after for CTAP.

Table 1 Magnetic resonance (MR) imaging parameters

Parameter	T_2-weighted imaging	T_1-weighted imaging	Contrast-enhanced MR imaging
Sequence	FSE	2D fast GRE	3D-GRE
Fat saturated	Yes	–	Yes
Respiratory triggered	Yes	–	–
Acquisition time	2 to 3 minutes	14 seconds	18 seconds
Repetition time	2500 to 8000 ms	150 to 170 ms	3 to 8 ms
Echo time	64 ms	2.2 and 4.5 ms	1.9 ms
Flip angle	90°	90°	12°
Parallel imaging factor	1.75	2	1
Number of excitations	1	1	1
Field of view (cm)	(32 to 40) × (32 to 40)	(32 to 40) × (32 to 40)	(35 to 42) × (40 to 45)
Matrix	256 × 192	256 × 160	320 × 192
Slice thickness	6	5	5
Inter-slice gap	0	0	-2.5
Others		Many cases required 2 breath holds.	Scan delay after administration, 20 to 30 seconds, one, 2, 5, 10, and 20 minutes.

FSE, fast spin echo; GRE, gradient echo; 2D, 2-dimensional; 3D, 3-dimensional

Determination of target nodules

Two radiologists with 11 and 13 years of experience in abdominal radiology reviewed all the EOB-MRI and CE-CT images to identify hypovascular nodules that showed hyperintensity (uptake of gadoxetic acid) on HP images. They selected nodules (1) delineated from the surrounding liver as round lesions with hyperintensity on both axial and sagittal HP images, (2) 5 mm or larger in maximum diameter, and (3) showing hypovascularity during hepatic arterial phase on EOB-MRI and CE-CT.

We excluded nodules that showed hyperintensity compared to the surrounding liver even on precontrast T_1WI regardless of their uptake of gadoxetic acid, because of the difficulty or impossibility of precisely determining a lack of contrast enhancement on hepatic arterial phase images of EOB-MRI and of detecting hypervascularization on follow-up hepatic arterial phase images. Hypovascularity of the nodules was confirmed by the lack of intralesional contrast enhancement on hepatic arterial phase images of both EOB-MRI and CE-CT [21].

Baseline imaging characteristics of the target nodules

We visually classified the signal intensity of nodules on T_2WI as high or not compared with the signal of the liver parenchyma, categorized signal on T_1WI as hypointense if nodules showed low intensity on both in- and opposed-phase images, and considered decreased signal on opposed-phase T_1WI to represent a lipid component. Nodule size was defined as the maximum diameter in the axial plane as measured on HP images.

We performed longitudinal evaluation of the included nodules based on findings of follow-up (second as well as third and fourth, if available) EOB-MRI or CE-CT. The follow-up interval was 3 to 4 months according to the Japanese clinical guideline for the diagnosis and treatment of HCC [22]. Increase in nodule size by 3 mm on follow-up HP images of EOB-MRI indicated increased size during the follow-up period.

Endpoint

We applied the primary endpoint, the development of an arterial supply within the nodules (i.e., hypervascularization), only if HCC was subsequently diagnosed.

We initially confirmed hypervascularization within the nodules using follow-up hepatic arterial phase images of EOB-MRI or CE-CT and added CTHA and CTAP when hypervascularization was ambiguous on hepatic arterial phase with EOB-MRI or CE-CT [23]. If hypervascularization within the nodules could be confirmed with more than one modality, we recorded the earliest date at which hypervascularization within the nodules was confirmed on hepatic arterial phase images as the time of onset of the endpoint.

Statistical analyses

We used the Cox proportional hazard model for univariate analysis to examine the hazard ratios of potential risk factors for the development of HCC from the nodules and for multivariate analysis to test further those patient- and nodule-based variables that showed a significant hazard ratio on univariate analysis. We used Kaplan-Meier time-to-event curves with 95 % confidence interval to estimate the cumulative risk for HCC to develop from the nodules and the log-rank test to compare the curves between those nodules with maximum diameters of 10 mm and larger and those smaller than 10 mm. Data analysis was performed using R version 3.1.2, with a 2-sided $p < 0.05$ considered to be statistically significant.

Results

Hypervascularization and clinical diagnosis of hepatocellular carcinoma

We observed hypervascularization in six of the 633 nodules (0.9 %) during the follow-up period. Two nodules clearly demonstrated hypervascularization on hepatic arterial phase of CE-CT. Four nodules required additional CTHA and CTAP to confirm hypervascularization that was ambiguous on the hepatic arterial phase of either CE-CT (one case) or EOB-MRI (one case), or both (two cases). All the hypervascularized nodules were clinically diagnosed as HCCs. Three nodules that fulfilled the criteria of wash-in and wash-out on CE-CT proposed by the American Association for the Study of Liver Disease (AASLD) [24] and European Association for the Study of the Liver [25] were treated with transcatheter chemoembolization. Three other nodules that showed hypervascularity on CTHA and decreased portal perfusion on CTAP [26–28] were treated with transcatheter chemoembolization using iodized oil, with confirmation of oil accumulation a week after treatment [29]. The median time to hypervascularization was 679 days (range, 110 to 1150 days).

Risk factors

Univariate analysis showed no patient-based factor as a risk for the development of hypervascular HCC from target nodules (Table 2). Of the 633 nodules, 39 increased in size (mean increase, 4.6 mm; range, 3 to 16 mm). Nodule-based univariate analyses associated a significant risk for HCC to develop with large nodule size at initial

Table 2 Univariate analysis: patient-based results

	Hypervascularization		Hazard ratio (95 % confidence interval)	*p* value
	+ (n = 5)	- (n = 64)		
Age (years)	66.8 ± 6.1	68.2 ± 10.0	1.00 (0.92 to 1.10)	0.974
Male	80 % (4/5)	53 % (34/64)	3.20 (0.35 to 28.93)	0.301
History of HCC	60 % (3/5)	50 % (32/64)	1.85 (0.31 to 11.10)	0.500
Concomitant HCC	60 % (3/5)	64 % (41/64)	1.11 (0.18 to 6.63)	0.913
Child-Pugh Class A	60 % (3/5)	56 % (36/64)	1.01 (0.17 to 6.05)	0.992
HCV	40 % (2/5)	70 % (45/64)	0.25 (0.04 to1.49)	0.128
HBV	40 % (2/5)	14 % (9/64)	4.19 (0.70 to 25.18)	0.118
Albumin level (g/dL)	3.86 ± 0.53	3.60 ± 0.49	2.73 (0.37 to 20.17)	0.324
Total bilirubin (mg/dL)	1.02 ± 0.29	0.95 ± 0.37	0.87 (0.08 to 8.88)	0.904
Prothrombin ratio (%)	63.7 ± 5.8	70.1 ± 9.6	0.93 (0.85 to 1.03)	0.174
Platelet count (10^9/L)	69.6 ± 20.3	88.5 ± 35.7	1.00 (1.00 to 1.00)	0.486
ICG-15 (%)	24.3 ± 7.4	25.0 ± 10.8	0.98 (0.89 to 1.08)	0.670
AFP > 15 ng/mL	40 % (2/5)	39 % (25/64)	1.60 (0.26 to 9.65)	0.609
PIVKA-II >40 mAU/mL	20 % (1/5)	20 % (13/64)	1.48 (0.16 to 13.37)	0.730

AFP, alpha-fetoprotein; HBV, hepatitis B virus; HCC, hepatocellular carcinoma; HCV, hepatitis C virus; ICG-15, retention of indocyanine green after 15 minutes; PIVKA-II, protein induced by vitamin K absence or antagonist II

examination (hazard ratio [95 % confidence interval [CI], 1.33 [1.17 to 1.51]), increase in nodule size during the follow-up period (hazard ratio [95 % CI], 8.30 [1.68 to 41.14]), and high signal intensity of nodules on T_2WI (hazard ratio [95 % CI], 11.50 [2.10 to 62.93]). Multivariate Cox analysis indicated nodule size at first examination ($p = 0.009$) as the only independent risk factor for the development of hypervascular HCC, with an odds ratio of 1.25 (95 % CI, 1.06 to 1.47) (Table 3). No nodule showed low signal intensity on T_1WI or evidence of lipid content.

The cutoff size of 10 mm corresponded with 100 % (6/6) sensitivity and 73.5 % (461/627) specificity to discriminate nodules with and without development of hypervascular HCC.

Cumulative risk of the development of hepatocellular carcinoma from the target nodule

At one year, the patient-based risk was 4.08 % (95 % CI, 1.74 to 9.55), and the nodule-based risk was 0.44 % (95 % CI, 0.20 to 0.95). The Kaplan-Meier curves differed significantly for nodules 10 mm and larger and those smaller than 10 mm ($p = 0.0022$; Fig. 2). The one-year risk of developing hypervascular HCC was 1.31 % [0.56 to 3.07] for the larger

Table 3 Univariate and multivariate analyses: nodule-based results

	Hypervascularization		Hazard ratio (95 % confidence interval)			
	+ (n = 6)	– (n = 627)	Univariate	*p* value	Multivariate	*p* value
Nodule size (SD) (mm)	16.0 (7.0)	8.3 (3.4)	1.33 (1.17 to 1.51)	<0.001	1.25 (1.06 to 1.47)	0.009
Increase in size	67 % (4/6)	9.2 % (58/627)	8.30 (1.68 to 41.14)	0.001	2.29 (0.30 to 17.51)	0.424
High signal intensity on T_2-weighted imaging	33 % (2/6)	2.7 % (17/627)	11.50 (2.10 to 62.93)	0.005	2.49 (0.29 to 21.03)	0.403

Nodule size is the size at initial magnetic resonance examination. Increase in size means an increase of 3 mm or more during follow-up. SD, standard deviation

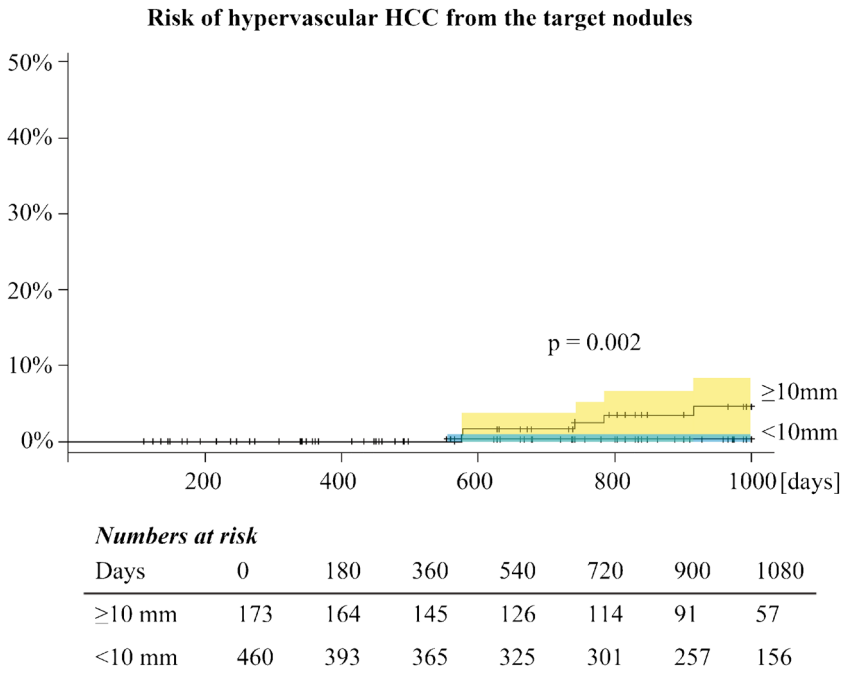

Numbers at risk

Days	0	180	360	540	720	900	1080
≥10 mm	173	164	145	126	114	91	57
<10 mm	460	393	365	325	301	257	156

Fig. 2 Longitudinal rates of hypervascular hepatocellular carcinoma (HCC) developing from target nodules (hypovascular nodules that showed uptake of gadoxetic acid on hepatocyte-phase images). Nodules with maximum diameters of 10 mm and larger showed significantly higher incidence of HCC development over time than those smaller than 10 mm ($p = 0.002$). However, even the larger nodules developed no HCC for the first year, which suggests no need to intensify follow-up for these nodules

nodules and only 0.10 % [0.02 to 0.57] for those smaller than 10 mm (Figs. 2 and 3).

Discussion

This retrospective longitudinal study revealed that hypovascular hepatic nodules that showed hyperintensity on gadoxetic acid-enhanced HP images rarely developed into hypervascular HCC. Though the risk was higher for larger nodules, we observed a low risk even for those measuring 10 mm and larger.

Arterial-phase imaging of the cirrhotic liver may demonstrate numerous hypovascular nodules, including regenerative and dysplastic nodules and early HCC [1]. Hypointensity on gadoxetic-acid HP images has been well reported as an indicator of malignancy or HCC [12, 13, 30] or at least high-grade dysplastic nodule [31]. The one-year risk of hypervascular HCC developing within a hypovascular nodule that shows hypointensity on initial HP images ranges from 15.6 to

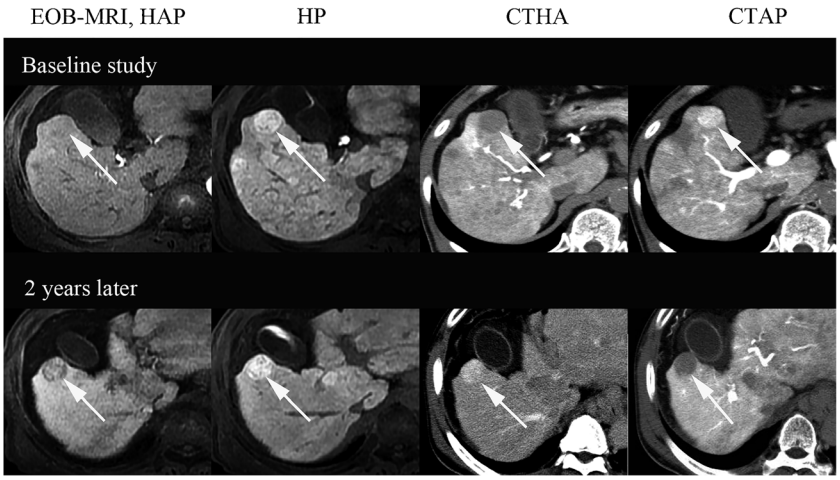

Fig. 3 A 67-year-old man with a hypervascularized nodule after 2 years of follow-up. Top images are baseline studies (initial gadoxetic acid-enhanced magnetic resonance imaging [EOB-MRI] and computed tomography during hepatic arteriography and arterial portography [CTHA/CTAP] around the same time). The nodule with 24-mm diameter is hypovascular on hepatic arterial phase images of EOB-MRI and CTHA (arrow) and showed hyperintensity on hepatocyte phase (HP) images. Two years later (bottom images); hypervascularization was apparent within the nodule (*arrow*), which was confirmed on CTHA. Decreased portal perfusion in the nodule, i.e. hypodensity on CTAP, suggests the development of hypervascular hepatocellular carcinoma

77.3 % [14–17, 19]. We found the risk minimal for hypovascular nodules that showed hyperintensity on HP images compared with those showing hypointensity. Further, the reported risk for the development of HCC in the cirrhotic liver (even without nodules) is around 8 % at one year [32] and 13 % at 3 years [33] in patients with no previous HCC. The AASLD guidelines for the management of HCC recommend ultrasonographic screening of cirrhotic liver every 6 months [24]. Considering the low risk we observed for the development of HCC from the target nodule, we believe these hypovascular, hyperintense nodules require neither treatment nor extensive follow-up beyond the AASLD recommendations.

HCCs typically show hypointensity on HP images [34], but this is not always the case [35]. The signal intensity of HCC during HP is well correlated with the expression of organic anion transporter (OATP) [36]. Recent publications revealed the favorable prognoses of some typical (hypervascular) HCCs that expressed OATP on the surface of tumour cells and showed hyperintensity during HP imaging [37, 38]. Although hypovascular HCCs can show increased uptake of gadoxetic acid during HP [20], our results suggest its uptake indicates favorable outcomes.

Our univariate analysis showed no patient-based factor as a risk for the development of hypervascular HCC from target nodules, though others have associated patient-based factors with both occurrence or recurrence of HCC [39–43]. Indeed, previous local therapy for HCC, Child-Pugh Class B cirrhosis, and coexistence of hypervascular HCC have been associated with an increased risk of hypervascularization in hypovascular nodules that demonstrated hypointensity on HP images [16]. Thus, we supposed that hypervascularization might be less aggressive in those hypovascular nodules with uptake of gadoxetic acid than those without. This point requires further investigation.

Our study has several limitations, including its retrospective design, which yielded varying intervals of imaging-based follow-up, and our relatively small number of patients, some with multiple nodules that produced a clustering effect in nodule-based results. Nevertheless, our consistent results in patient- and nodule-based analyses may indicate that any clustering effect was minimal.

In conclusion, hypovascular, hyperintense hepatic nodules rarely develop into hypervascular hepatocellular carcinomas. Though that risk is higher for larger nodules, even those 10 mm and larger require no altered management for patients with cirrhosis.

Acknowledgments The scientific guarantor of this publication is Tomoaki Ichikawa. The authors of this manuscript declare no relationships with any companies, whose products or services may be related to the subject matter of the article. The authors state that this work has not received any funding.

No complex statistical methods were necessary for this paper. Institutional Review Board approval was obtained. Written informed consent was waived by the Institutional Review Board.

Methodology: retrospective, diagnostic study, performed at one institution.

References

1. International Consensus Group for Hepatocellular Neoplasia (2009) Pathologic diagnosis of early hepatocellular carcinoma: a report of the International Consensus Group for Hepatocellular Neoplasia. Hepatology 49:658–664
2. Takayama T, Makuuchi M, Hirohashi S et al (1990) Malignant transformation of adenomatous hyperplasia to hepatocellular carcinoma. Lancet 336:1150–1153
3. Kitao A, Zen Y, Matsui O, Gabata T, Nakanuma Y (2009) Hepatocarcinogenesis: multistep changes of drainage vessels at CT during arterial portography and hepatic arteriography–radiologic-pathologic correlation. Radiology 252:605–614
4. Huppertz A, Haraida S, Kraus A et al (2005) Enhancement of focal liver lesions at gadoxetic acid-enhanced MR imaging: correlation with histopathologic findings and spiral CT–initial observations. Radiology 234:468–478
5. Motosugi U, Ichikawa T, Sou H et al (2010) Distinguishing hypervascular pseudolesions of the liver from hypervascular hepatocellular carcinomas with gadoxetic acid-enhanced MR imaging. Radiology 256:151–158
6. Jung G, Breuer J, Poll LW et al (2006) Imaging characteristics of hepatocellular carcinoma using the hepatobiliary contrast agent Gd-EOB-DTPA. Acta Radiol 47:15–23
7. Neri E, Bali MA, Ba-Ssalamah A et al (2016) ESGAR consensus statement on liver MR imaging and clinical use of liver-specific contrast agents. Eur Radiol 26:921–931
8. Ahn SS, Kim MJ, Lim JS, Hong HS, Chung YE, Choi JY (2010) Added value of gadoxetic acid-enhanced hepatobiliary phase MR imaging in the diagnosis of hepatocellular carcinoma. Radiology 255:459–466
9. Motosugi U, Ichikawa T, Araki T (2013) Rules, roles, and room for discussion in gadoxetic acid-enhanced magnetic resonance liver imaging: current knowledge and future challenges. Magn Reson Med Sci 12:161–175
10. Inoue T, Kudo M, Komuta M et al (2012) Assessment of Gd-EOB-DTPA-enhanced MRI for HCC and dysplastic nodules and comparison of detection sensitivity versus MDCT. J Gastroenterol 47:1036–1047
11. Ichikawa T, Saito K, Yoshioka N et al (2010) Detection and characterization of focal liver lesions: a Japanese phase III, multicenter comparison between gadoxetic acid disodium-enhanced magnetic resonance imaging and contrast-enhanced computed tomography predominantly in patients with hepatocellular carcinoma and chronic liver disease. Investig Radiol 45:133–141
12. Golfieri R, Grazioli L, Orlando E et al (2012) Which is the best MRI marker of malignancy for atypical cirrhotic nodules: hypointensity in hepatobiliary phase alone or combined with other features? Classification after Gd-EOB-DTPA administration. J Magn Reson Imaging 36:648–657
13. Sano K, Ichikawa T, Motosugi U et al (2011) Imaging study of early hepatocellular carcinoma: usefulness of gadoxetic acid-enhanced MR imaging. Radiology 261:834–844
14. Motosugi U, Ichikawa T, Sano K et al (2011) Outcome of hypovascular hepatic nodules revealing no gadoxetic acid uptake in patients with chronic liver disease. J Magn Reson Imaging 34:88–94

15. Kumada T, Toyoda H, Tada T et al (2011) Evolution of hypointense hepatocellular nodules observed only in the hepatobiliary phase of gadoxetate disodium-enhanced MRI. AJR Am J Roentgenol 197: 58–63
16. Hyodo T, Murakami T, Imai Y et al (2013) Hypovascular nodules in patients with chronic liver disease: risk factors for development of hypervascular hepatocellular carcinoma. Radiology 266:480–490
17. Kim YK, Lee WJ, Park MJ, Kim SH, Rhim H, Choi D (2012) Hypovascular hypointense nodules on hepatobiliary phase gadoxetic acid-enhanced MR images in patients with cirrhosis: potential of DW imaging in predicting progression to hypervascular HCC. Radiology 265:104–114
18. Kim YS, Song JS, Lee HK, Han YM (2015) Hypovascular hypointense nodules on hepatobiliary phase without T2 hyperintensity on gadoxetic acid-enhanced MR images in patients with chronic liver disease: long-term outcomes and risk factors for hypervascular transformation. Eur Radiol. doi:10.1007/s00330-015-4146-9
19. Higaki A, Ito K, Tamada T et al (2014) Prognosis of small hepatocellular nodules detected only at the hepatobiliary phase of Gd-EOB-DTPA-enhanced MR imaging as hypointensity in cirrhosis or chronic hepatitis. Eur Radiol 24:2476–2481
20. Chen N, Motosugi U, Sano K et al (2013) Early hepatocellular carcinomas showing isointensity or hyperintensity in gadoxetic acid-enhanced, hepatocyte-phase magnetic resonance images. J Comput Assist Tomogr 37:466–469
21. Kanata N, Yoshikawa T, Ohno Y et al (2013) HCC-to-liver contrast on arterial-dominant phase images of EOB-enhanced MRI: comparison with dynamic CT. Magn Reson Imaging 31:17–22
22. Kudo M, Matsui O, Izumi N, Iijima H, Kadoya M, Imai Y (2014) Surveillance and diagnostic algorithm for hepatocellular carcinoma proposed by the Liver Cancer Study Group of Japan: 2014 update. Oncology 87:7–21
23. Imai Y, Murakami T, Hori M et al (2008) Hypervascular hepatocellular carcinoma: combined dynamic MDCT and SPIO-enhanced MRI versus combined CTHA and CTAP. Hepatol Res 38:147–158
24. Bruix J, Sherman M, American Association for the Study of Liver Diseases (2011) Management of hepatocellular carcinoma: an update. Hepatology 53:1020–1022
25. European Association for the Study of the Liver, European Organisation for Research and Treatment of Cancer (2012) EASL-EORTC clinical practice guidelines: management of hepatocellular carcinoma. J Hepatol 56:908–943
26. Murakami T, Oi H, Hori M et al (1997) Helical CT during arterial portography and hepatic arteriography for detecting hypervascular hepatocellular carcinoma. AJR Am J Roentgenol 169:131–135
27. Matsui O, Takashima T, Kadoya M et al (1985) Dynamic computed tomography during arterial portography: the most sensitive examination for small hepatocellular carcinomas. J Comput Assist Tomogr 9:19–24
28. Miyayama S, Matsui O, Yamashiro M et al (2009) Detection of hepatocellular carcinoma by CT during arterial portography using a cone-beam CT technology: comparison with conventional CTAP. Abdom Imaging 34:502–506
29. Merine D, Takayasu K, Wakao F (1990) Detection of hepatocellular carcinoma: comparison of CT during arterial portography with CT after intraarterial injection of iodized oil. Radiology 175:707–710
30. Van Beers BE, Pastor CM, Hussain HK (2012) Primovist, Eovist: what to expect? J Hepatol 57:421–429
31. Bartolozzi C, Battaglia V, Bargellini I et al (2013) Contrast-enhanced magnetic resonance imaging of 102 nodules in cirrhosis: correlation with histological findings on explanted livers. Abdom Imaging 38:290–296
32. Yoshida H, Shiratori Y, Moriyama M et al (1999) Interferon therapy reduces the risk for hepatocellular carcinoma: national surveillance program of cirrhotic and noncirrhotic patients with chronic hepatitis C in Japan. IHIT Study Group. Inhibition of Hepatocarcinogenesis by Interferon Therapy. Ann Intern Med 131:174–181
33. Tsukuma H, Hiyama T, Tanaka S et al (1993) Risk factors for hepatocellular carcinoma among patients with chronic liver disease. N Engl J Med 328:1797–1801
34. Motosugi U, Bannas P, Sano K, Reeder SB (2015) Hepatobiliary MR contrast agents in hypovascular hepatocellular carcinoma. J Magn Reson Imaging 41:251–265
35. Tsuboyama T, Onishi H, Kim T et al (2010) Hepatocellular carcinoma: hepatocyte-selective enhancement at gadoxetic acid-enhanced MR imaging–correlation with expression of sinusoidal and canalicular transporters and bile accumulation. Radiology 255:824–833
36. Kitao A, Zen Y, Matsui O et al (2010) Hepatocellular carcinoma: signal intensity at gadoxetic acid-enhanced MR imaging–correlation with molecular transporters and histopathologic features. Radiology 256:817–826
37. Kitao A, Matsui O, Yoneda N et al (2012) Hypervascular hepatocellular carcinoma: correlation between biologic features and signal intensity on gadoxetic acid-enhanced MR images. Radiology 265: 780–789
38. Choi JW, Lee JM, Kim SJ et al (2013) Hepatocellular carcinoma: imaging patterns on gadoxetic acid-enhanced MR images and their value as an imaging biomarker. Radiology 267:776–786
39. Beasley RP, Hwang LY, Lin CC, Chien CS (1981) Hepatocellular carcinoma and hepatitis B virus. A prospective study of 22 707 men in Taiwan. Lancet 2:1129–1133
40. Liang TJ, Jeffers LJ, Reddy KR et al (1993) Viral pathogenesis of hepatocellular carcinoma in the United States. Hepatology 18: 1326–1333
41. Tateishi R, Yoshida H, Matsuyama Y, Mine N, Kondo Y, Omata M (2008) Diagnostic accuracy of tumor markers for hepatocellular carcinoma: a systematic review. Hepatol Int 2:17–30
42. Chang KC, Lu SN, Chen PF et al (2011) Incidence and associated risk factors of hepatocellular carcinoma in a dural hepatitis B and C virus endemic area: a surveillance study. Kaohsiung J Med Sci 27: 85–90
43. Lok AS, Seeff LB, Morgan TR et al (2009) Incidence of hepatocellular carcinoma and associated risk factors in hepatitis C-related advanced liver disease. Gastroenterology 136:138–148